DTP/00/70,IPPP/00/08,MADPH-00-1200,hep-ph/0011094

Two-loop QCD corrections to massless identical quark scattering*

C. Anastasiou[a], **E. W. N. Glover**[a], **C. Oleari**[b] **and M. E. Tejeda-Yeomans**[a]

[a] *Department of Physics, University of Durham, Durham DH1 3LE, England*

[b] *Department of Physics, University of Wisconsin, 1150 University Avenue Madison WI 53706, U.S.A.*

E-mail: Ch.Anastasiou@durham.ac.uk, E.W.N.Glover@durham.ac.uk, Oleari@pheno.physics.wisc.edu, M.E.Tejeda-Yeomans@durham.ac.uk

Abstract: We present the two-loop virtual QCD corrections to the scattering of identical massless quarks, $q\bar{q} \to q\bar{q}$, in conventional dimensional regularisation and using the $\overline{\mathrm{MS}}$ scheme. The structure of the infrared divergences agrees with that predicted by Catani while expressions for the finite remainder are given for the $q\bar{q} \to q\bar{q}$ and the $qq \to qq$ ($\bar{q}\bar{q} \to \bar{q}\bar{q}$) scattering processes in terms of polylogarithms. The results presented here form a vital part of the next-to-next-to-leading order contribution to inclusive jet production in hadron colliders and will play a crucial role in improving the theoretical prediction for jet cross sections in hadron-hadron collisions.

Keywords: QCD, Jets, LEP HERA and SLC Physics, NLO and NNLO Computations.

*Work supported in part by the UK Particle Physics and Astronomy Research Council and by the EU Fourth Framework Programme 'Training and Mobility of Researchers', Network 'Quantum Chromodynamics and the Deep Structure of Elementary Particles', contract FMRX-CT98-0194 (DG 12 - MIHT). C.A. acknowledges the financial support of the Greek government and M.E.T. acknowledges financial support from CONACyT and the CVCP. We thank the British Council and German Academic Exchange Service for support under ARC project 1050.

1. Introduction

Jet production at large transverse energies is a direct test of parton-parton scattering processes in hadron-hadron collisions. At large jet energy scales, the point-like nature of the partons can be probed down to distance scales of about 10^{-17} m by comparing data with QCD predictions. Within the experimental and theoretical uncertainties, data from the TEVATRON and CERN S$p\bar{p}$S generally show good agreement with the state-of-the-art theoretical next-to-leading order $\mathcal{O}(\alpha_s^3)$ estimates based on massless parton-parton scattering over a wide range of jet energies [1, 2]. It is anticipated that the forthcoming Run II starting at the TEVATRON in 2001 will yield a dramatic improvement in the quality of the data with increased statistics and improved detectors, leading to a significant reduction in both the statistical and systematic errors. Subsequently, the start of data taking at the LHC will lead to a much enlarged range of jet energies being probed.

It is a challenge to the physics community to improve the quality of the theoretical predictions to a level that matches the improved experimental accuracy. This may be achieved by including the next-to-next-to-leading order QCD corrections which both reduces the renormalisation scale dependence and improves the matching of the parton-level theoretical jet algorithm with the hadron-level experimental jet algorithm.

The full next-to-next-to-leading order prediction is a formidable task and requires a knowledge of the two-loop $2 \to 2$ matrix elements as well as the contributions from the one-loop $2 \to 3$ and tree-level $2 \to 4$ processes. In the interesting large-transverse-energy region, $E_T \gg m_{\text{quark}}$, the quark masses may be safely neglected and we therefore focus on the scattering of massless partons. For processes involving up, down and strange quarks, which together with processes involving gluons form the bulk of the cross section, this is certainly a reliable approximation. The contribution involving charm and bottom quarks is only a small part of the total since the parton densities for finding charm and bottom quarks inside the proton are relatively suppressed. We note that the existing next-to-leading order programs [1, 2] used to compare directly with the experimental jet data [3, 4] are based on massless parton-parton scattering. Helicity amplitudes for the one-loop $2 \to 3$ parton sub-processes have been computed in [5, 6, 7] while the amplitudes for the tree-level $2 \to 4$ processes are available in [8, 9, 10, 11]. The parton-density functions are also needed to next-to-next-to-leading order accuracy. This requires knowledge of the three-loop splitting functions. At present, the even moments of the splitting functions are known for the flavour singlet and non-singlet structure functions F_2 and F_L up to $N = 12$ while the odd moments up to $N = 13$ are known for F_3 [12, 13]. The numerically small N_F^2 non-singlet contribution is also known [14]. Van Neerven and Vogt have provided accurate parameterisations of the splitting functions in x-space [15, 16] which are now starting to be implemented in the global analyses [17].

The calculation of the two-loop amplitudes for the $2 \to 2$ scattering of light-like particles has proved more intractable due mainly to the difficulty of evaluating the planar and non-planar double box graphs. Recently, however, analytic expressions for these basic scalar integrals have been provided by Smirnov [18] and Tausk [19] as series in $\epsilon = (4-D)/2$. Algorithms for computing the associated tensor integrals have also been provided [20] and [21], so that generic two-loop massless $2 \to 2$ processes can in principle be expressed in terms of a basis set of known two-loop integrals. Bern, Dixon and Kosower [22] were the first to address such scattering processes and provided analytic expressions for the maximal-helicity-violating two-loop amplitude for $gg \to gg$. Subsequently, Bern, Dixon and Ghinculov [23] completed the two-loop calculation of physical $2 \to 2$ scattering amplitudes for the QED processes $e^+e^- \to \mu^+\mu^-$ and $e^+e^- \to e^-e^+$.

In an earlier paper [24], we derived expressions for the two-loop contribution to unlike quark scattering, $q\bar{q} \to q'\bar{q}'$, as well as the crossed and time reversed processes. The infrared pole structure agreed with that predicted by Catani [25] and we provided explicit formulae for the finite parts in the s-, t- and u-channels in terms of logarithms and polylogarithms. Matrix elements for the other parton-parton scattering processes remain to be evaluated. In this paper we extend the work of [24] to describe the case of identical quark scattering. We use the $\overline{\rm MS}$ renormalisation scheme and conventional dimensional regularisation where all external particles are treated in D dimensions to provide dimensionally regularised and renormalised analytic expressions at the two-loop level for the scattering process

$$q\bar{q} \to q\bar{q},$$

together with the time-reversed and crossed processes

$$\begin{aligned} q + q &\to q + q, \\ \bar{q} + \bar{q} &\to \bar{q} + \bar{q}. \end{aligned}$$

As in the unlike quark case, we present analytic expressions for the infrared pole structure, as well as explicit formulae for the finite remainder decomposed according to powers of the number of colours N and the number of light-quark flavours N_F. For the contributions most subleading in N, there is an overlap with the two-loop contribution to Bhabha scattering described in [23] and the analytic expressions presented here provide a useful check of some of their results.

Our paper is organised as follows. We first establish our notation in Section 2. The results are collected in Section 3 where we provide analytic expressions for the interference of the two-loop and tree-level amplitudes as series expansions in ϵ. In Section 3.1 we adopt the notation of Catani [25] to isolate the infrared singularity structure of the two-loop amplitudes in the $\overline{\rm MS}$ scheme. We give explicit formulae for the pole structure obtained by direct evaluation of the Feynman diagrams and show that it agrees with the pole structure expected on general grounds. The finite $\mathcal{O}(\epsilon^0)$ remainder of the two-loop graphs is the main result of our paper and expressions appropriate for the $q\bar{q} \to q\bar{q}$ and $qq \to qq$ ($\bar{q}\bar{q} \to \bar{q}\bar{q}$) scattering processes are are given in Section 3.2. Finally Section 4 contains a brief summary of our results.

2. Notation

For calculational convenience, we treat all particles as incoming so that

$$q(p_1) + \bar{q}(p_2) + q(p_3) + \bar{q}(p_4) \to 0, \tag{2.1}$$

where the light-like momentum assignments are in parentheses and satisfy

$$p_1^\mu + p_2^\mu + p_3^\mu + p_4^\mu = 0.$$

As stated above, we work in conventional dimensional regularisation treating all external states in D dimensions. We renormalise in the $\overline{\text{MS}}$ scheme where the bare coupling α_0 is related to the running coupling $\alpha_s \equiv \alpha_s(\mu^2)$ at renormalisation scale μ via

$$\alpha_0 \, S_\epsilon = \alpha_s \left[1 - \frac{\beta_0}{\epsilon}\left(\frac{\alpha_s}{2\pi}\right) + \left(\frac{\beta_0^2}{\epsilon^2} - \frac{\beta_1}{2\epsilon}\right)\left(\frac{\alpha_s}{2\pi}\right)^2 + \mathcal{O}\left(\alpha_s^3\right)\right]. \tag{2.2}$$

In this expression

$$S_\epsilon = (4\pi)^\epsilon e^{-\epsilon\gamma}, \qquad \gamma = 0.5772\ldots = \text{Euler constant} \tag{2.3}$$

is the typical phase-space volume factor in $D = 4 - 2\epsilon$ dimensions, and β_0, β_1 are the first two coefficients of the QCD beta function for N_F (massless) quark flavours

$$\beta_0 = \frac{11C_A - 4T_R N_F}{6}\ , \qquad \beta_1 = \frac{17C_A^2 - 10C_A T_R N_F - 6C_F T_R N_F}{6}\ . \tag{2.4}$$

For an $SU(N)$ gauge theory (N is the number of colours)

$$C_F = \left(\frac{N^2-1}{2N}\right), \qquad C_A = N, \qquad T_R = \frac{1}{2}. \tag{2.5}$$

The renormalised four point amplitude in the $\overline{\text{MS}}$ scheme is thus

$$\begin{aligned}|\mathcal{M}\rangle = 4\pi\alpha_s \Bigg[&\left(|\mathcal{M}^{(0)}\rangle - |\overline{\mathcal{M}}^{(0)}\rangle\right) + \left(\frac{\alpha_s}{2\pi}\right)\left(|\mathcal{M}^{(1)}\rangle - |\overline{\mathcal{M}}^{(1)}\rangle\right) \\ &+ \left(\frac{\alpha_s}{2\pi}\right)^2\left(|\mathcal{M}^{(2)}\rangle - |\overline{\mathcal{M}}^{(2)}\rangle\right) + \mathcal{O}\left(\alpha_s^3\right)\Bigg],\end{aligned} \tag{2.6}$$

where the $|\mathcal{M}^{(i)}\rangle$ represents the colour-space vector describing the i-loop amplitude for the s-channel graphs, and the t-channel contribution $|\overline{\mathcal{M}}^{(i)}\rangle$ is obtained by exchanging the roles of particles 2 and 4:

$$|\overline{\mathcal{M}}^{(i)}\rangle = |\mathcal{M}^{(i)}\rangle(2 \leftrightarrow 4). \tag{2.7}$$

The dependence on both renormalisation scale μ and renormalisation scheme is implicit.

We denote the squared amplitude summed over spins and colours by

$$\begin{aligned}\langle\mathcal{M}|\mathcal{M}\rangle &= \sum|\mathcal{M}(q+\bar{q}\to\bar{q}+q)|^2 \\ &= \mathcal{A}(s,t,u)+\mathcal{A}(t,s,u)+\mathcal{B}(s,t,u),\end{aligned} \tag{2.8}$$

where the Mandelstam variables are given by

$$s=(p_1+p_2)^2, \qquad t=(p_2+p_3)^2, \qquad u=(p_1+p_3)^2. \tag{2.9}$$

The squared matrix elements for the $qq\to qq$ process are obtained by exchanging s and u

$$\sum|\mathcal{M}(q+q\to q+q)|^2=\mathcal{A}(u,t,s)+\mathcal{A}(t,u,s)+\mathcal{B}(u,t,s). \tag{2.10}$$

The function $\mathcal{A}$ is related to the squared matrix elements for unlike quark scattering

$$\mathcal{A}(s,t,u)=\sum|\mathcal{M}(q+\bar{q}\to\bar{q}'+q')|^2 \tag{2.11}$$

$$\mathcal{A}(t,s,u)=\sum|\mathcal{M}(q+\bar{q}'\to\bar{q}'+q)|^2 \tag{2.12}$$

while $\mathcal{B}(s,t,u)$ represents the interference between s-channel and t-channel graphs that is only present for identical quark scattering.

The function $\mathcal{A}$ can be expanded perturbatively to yield

$$\mathcal{A}(s,t,u)=16\pi^2\alpha_s^2\left[\mathcal{A}^4(s,t,u)+\left(\frac{\alpha_s}{2\pi}\right)\mathcal{A}^6(s,t,u)+\left(\frac{\alpha_s}{2\pi}\right)^2\mathcal{A}^8(s,t,u)+\mathcal{O}\left(\alpha_s^3\right)\right], \tag{2.13}$$

where

$$\mathcal{A}^4(s,t,u)=\langle\mathcal{M}^{(0)}|\mathcal{M}^{(0)}\rangle\equiv 2(N^2-1)\left(\frac{t^2+u^2}{s^2}-\epsilon\right), \tag{2.14}$$

$$\mathcal{A}^6(s,t,u)=\left(\langle\mathcal{M}^{(0)}|\mathcal{M}^{(1)}\rangle+\langle\mathcal{M}^{(1)}|\mathcal{M}^{(0)}\rangle\right), \tag{2.15}$$

$$\mathcal{A}^8(s,t,u)=\left(\langle\mathcal{M}^{(1)}|\mathcal{M}^{(1)}\rangle+\langle\mathcal{M}^{(0)}|\mathcal{M}^{(2)}\rangle+\langle\mathcal{M}^{(2)}|\mathcal{M}^{(0)}\rangle\right). \tag{2.16}$$

Expressions for $\mathcal{A}^6$ are given in Ref. [26] using dimensional regularisation to isolate the infrared and ultraviolet singularities. Analytical formulae for the two-loop contribution to $\mathcal{A}^8$, $\langle\mathcal{M}^{(0)}|\mathcal{M}^{(2)}\rangle+\langle\mathcal{M}^{(2)}|\mathcal{M}^{(0)}\rangle$, are given in Ref. [24].

Similarly, the expansion of $\mathcal{B}$ can be written

$$\mathcal{B}(s,t,u)=16\pi^2\alpha_s^2\left[\mathcal{B}^4(s,t,u)+\left(\frac{\alpha_s}{2\pi}\right)\mathcal{B}^6(s,t,u)+\left(\frac{\alpha_s}{2\pi}\right)^2\mathcal{B}^8(s,t,u)+\mathcal{O}\left(\alpha_s^3\right)\right], \tag{2.17}$$

where, in terms of the amplitudes, we have

$$\begin{aligned}
\mathcal{B}^4(s,t,u) &= -\left(\langle\overline{\mathcal{M}}^{(0)}|\mathcal{M}^{(0)}\rangle + \langle\mathcal{M}^{(0)}|\overline{\mathcal{M}}^{(0)}\rangle\right) \\
&\equiv -4\left(\frac{N^2-1}{N}\right)(1-\epsilon)\left(\frac{u^2}{st}+\epsilon\right),
\end{aligned} \tag{2.18}$$

$$\mathcal{B}^6(s,t,u) = -\left(\langle\overline{\mathcal{M}}^{(1)}|\mathcal{M}^{(0)}\rangle + \langle\mathcal{M}^{(0)}|\overline{\mathcal{M}}^{(1)}\rangle + \langle\overline{\mathcal{M}}^{(0)}|\mathcal{M}^{(1)}\rangle + \langle\mathcal{M}^{(1)}|\overline{\mathcal{M}}^{(0)}\rangle\right) \tag{2.19}$$

$$\begin{aligned}
\mathcal{B}^8(s,t,u) = -\Big(&\langle\overline{\mathcal{M}}^{(1)}|\mathcal{M}^{(1)}\rangle + \langle\mathcal{M}^{(1)}|\overline{\mathcal{M}}^{(1)}\rangle \\
&+\langle\overline{\mathcal{M}}^{(0)}|\mathcal{M}^{(2)}\rangle + \langle\mathcal{M}^{(2)}|\overline{\mathcal{M}}^{(0)}\rangle + \langle\mathcal{M}^{(0)}|\overline{\mathcal{M}}^{(2)}\rangle + \langle\overline{\mathcal{M}}^{(2)}|\mathcal{M}^{(0)}\rangle\Big).
\end{aligned} \tag{2.20}$$

As before, expressions for $\mathcal{B}^6$ which are valid in conventional dimensional regularisation are given in Ref. [26]. Here, in order to complete the calculation of the two-loop contribution to quark-quark scattering, we concentrate on the next-to-next-to-leading order contribution $\mathcal{B}^8$ and in particular the interference of the two-loop and tree graphs.

As in Ref. [24], we use `QGRAF` [27] to produce the two-loop Feynman diagrams to construct either $|\mathcal{M}^{(2)}\rangle$ or $|\overline{\mathcal{M}}^{(2)}\rangle$. We then project by $\langle\overline{\mathcal{M}}^{(0)}|$ or $\langle\mathcal{M}^{(0)}|$ respectively and perform the summation over colours and spins. Finally, the trace over the Dirac matrices is carried out in D dimensions using conventional dimensional regularisation. It is then straightforward to identify the scalar and tensor integrals present and replace them with combinations of the basis set of master integrals using the tensor reduction of two-loop integrals described in [20, 21, 29], based on integration-by-parts [30] and Lorentz invariance [31] identities. The final result is a combination of master integrals in $D = 4-2\epsilon$. The basis set we choose comprises

$\mathrm{Sunset}(s) =$ 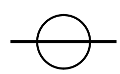 (s) (2.21)

$\mathrm{Glass}(s) =$ 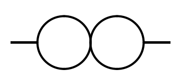 (s) (2.22)

$\mathrm{Tri}(s) =$ 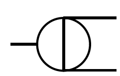 (s) (2.23)

$\mathrm{Abox}(s,t) =$ 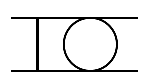 (s,t) (2.24)

$\mathrm{Cbox}(s,t) =$ 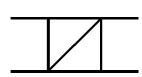 (s,t) (2.25)

$\mathrm{Pbox}_1(s,t) =$ 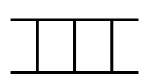 (s,t) (2.26)

$\mathrm{Xbox}_1(s,t) =$ 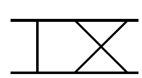 (s,t) (2.27)

$$\mathrm{Xbox}_2(s,t) = $$ 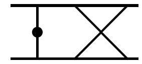 $$(s,t) \tag{2.28}$$

and[1]

$$\mathrm{Pbox}_3(s,t) = $$ 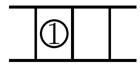 $$(s,t), \tag{2.29}$$

where ① represents the planar box integral with one irreducible numerator associated with the left loop. The expansion in ϵ for all the non-trivial master integrals can be found in [18, 19, 20, 21, 28, 29, 33, 34, 35].

3. Results

In this section, we give explicit formulae for the ϵ-expansion of the two-loop contribution to the next-to-next-to-leading order term $\mathcal{B}^8(s,t,u)$. To distinguish between the genuine two-loop contribution and the squared one-loop part, we decompose $\mathcal{B}^8$ as

$$\mathcal{B}^8 = \mathcal{B}^{8\ (2\times 0)} + \mathcal{B}^{8\ (1\times 1)}. \tag{3.1}$$

The one-loop-square contribution $\mathcal{B}^{8\ (1\times 1)}$ is vital in determining $\mathcal{B}^8$ but is relatively straightforward to obtain. For the remainder of this paper we concentrate on the technically more complicated two-loop contribution $\mathcal{B}^{8\ (2\times 0)}$.

As in Ref. [24], we divide the two-loop contributions into two classes: those that multiply poles in the dimensional regularisation parameter ϵ and those that are finite as $\epsilon \to 0$

$$\mathcal{B}^{8\ (2\times 0)}(s,t,u) = \mathcal{P}oles + \mathcal{F}inite. \tag{3.2}$$

$\mathcal{P}oles$ contains infrared singularities that will be analytically canceled by the infrared singularities occurring in radiative processes of the same order (ultraviolet divergences are removed by renormalisation).

[1]Reference [20] describes the procedure for reducing the tensor integrals down to a basis involving the planar box integral

$$\mathrm{Pbox}_2(s,t) = $$ 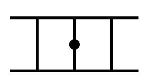 $$(s,t)\ ,$$

where the blob on the middle propagator represents an additional power of that propagator, and provides a series expansion for Pbox_2 to $\mathcal{O}\left(\epsilon^0\right)$. However, as was pointed out in [32], knowledge of Pbox_1 and Pbox_2 to $\mathcal{O}\left(\epsilon^0\right)$ is not sufficient to determine all tensor loop integrals to the same order. Series expansions for Pbox_3 are relatively compact and straightforward to obtain and are detailed in [34, 35]. Pbox_2 can therefore be eliminated in favor of Pbox_3. We note that this choice is not unique. Bern et al. [23] choose to use the Pbox_1 and Pbox_2 basis, but with the integrals evaluated in $D = 6-2\epsilon$ dimensions where they are both infrared and ultraviolet finite.

3.1 Infrared Pole Structure

Catani has made predictions for the singular infrared behaviour of two-loop amplitudes. Following the procedure advocated in [25], we find that the pole structure in the $\overline{\rm MS}$ scheme can be written as

$$\begin{aligned}\mathcal{P}oles = -2\,{\rm Re}\Bigg[& \frac{1}{2}\langle\overline{\mathcal{M}}^{(0)}|\boldsymbol{I}^{(1)}(\epsilon)\boldsymbol{I}^{(1)}(\epsilon)|\mathcal{M}^{(0)}\rangle - \frac{\beta_0}{\epsilon}\langle\overline{\mathcal{M}}^{(0)}|\boldsymbol{I}^{(1)}(\epsilon)|\mathcal{M}^{(0)}\rangle \\ & + \langle\overline{\mathcal{M}}^{(0)}|\boldsymbol{I}^{(1)}(\epsilon)|\mathcal{M}^{(1){\rm fin}}\rangle \\ & + e^{-\epsilon\gamma}\frac{\Gamma(1-2\epsilon)}{\Gamma(1-\epsilon)}\left(\frac{\beta_0}{\epsilon}+K\right)\langle\overline{\mathcal{M}}^{(0)}|\boldsymbol{I}^{(1)}(2\epsilon)|\mathcal{M}^{(0)}\rangle \\ & + \langle\overline{\mathcal{M}}^{(0)}|\boldsymbol{H}^{(2)}(\epsilon)|\mathcal{M}^{(0)}\rangle + (s\leftrightarrow t)\Bigg],\end{aligned} \tag{3.3}$$

where the constant K is

$$K = \left(\frac{67}{18}-\frac{\pi^2}{6}\right)C_A - \frac{10}{9}T_R N_F. \tag{3.4}$$

In Eq. (3.3), the symmetrisation under s and t exchange represents the additional effect of the s-channel tree graph interfering with the t-channel two-loop graphs.

The colour algebra is straightforward and we find that the s-t symmetric contributions proportional to

$$\langle\overline{\mathcal{M}}^{(0)}|\mathcal{M}^{(0)}\rangle = 2\left(\frac{N^2-1}{N}\right)(1-\epsilon)\left(\frac{u^2}{st}+\epsilon\right), \tag{3.5}$$

are given by

$$\begin{aligned}&\langle\overline{\mathcal{M}}^{(0)}|\boldsymbol{I}^{(1)}(\epsilon)|\mathcal{M}^{(0)}\rangle = \langle\overline{\mathcal{M}}^{(0)}|\mathcal{M}^{(0)}\rangle \\ &\times\frac{e^{\epsilon\gamma}}{\Gamma(1-\epsilon)}\left(\frac{1}{\epsilon^2}+\frac{3}{2\epsilon}\right)\left[\frac{1}{N}\left(-\frac{\mu^2}{s}\right)^{\epsilon}+\frac{1}{N}\left(-\frac{\mu^2}{t}\right)^{\epsilon}-\frac{N^2+1}{N}\left(-\frac{\mu^2}{u}\right)^{\epsilon}\right]\end{aligned} \tag{3.6}$$

$$\begin{aligned}&\langle\overline{\mathcal{M}}^{(0)}|\boldsymbol{I}^{(1)}(\epsilon)\boldsymbol{I}^{(1)}(\epsilon)|\mathcal{M}^{(0)}\rangle = \langle\overline{\mathcal{M}}^{(0)}|\mathcal{M}^{(0)}\rangle \\ &\times\frac{e^{2\epsilon\gamma}}{\Gamma(1-\epsilon)^2}\left(\frac{1}{\epsilon^2}+\frac{3}{2\epsilon}\right)^2\Bigg\{\frac{N^4-3N^2-2}{N^2}\left(-\frac{\mu^2}{u}\right)^{\epsilon}\left[\left(-\frac{\mu^2}{s}\right)^{\epsilon}+\left(-\frac{\mu^2}{t}\right)^{\epsilon}\right] \\ &\quad+\frac{3N^2+1}{N^2}\left(-\frac{\mu^2}{u}\right)^{2\epsilon}-\frac{(N^2-2)(N^2+1)}{N^2}\left(-\frac{\mu^2}{s}\right)^{\epsilon}\left(-\frac{\mu^2}{t}\right)^{\epsilon} \\ &\quad+\frac{1}{N^2}\left(-\frac{\mu^2}{s}\right)^{2\epsilon}+\frac{1}{N^2}\left(-\frac{\mu^2}{t}\right)^{2\epsilon}\Bigg\}\end{aligned} \tag{3.7}$$

and

$$\begin{aligned}&\langle\overline{\mathcal{M}}^{(0)}|\boldsymbol{H}^{(2)}(\epsilon)|\mathcal{M}^{(0)}\rangle = \langle\overline{\mathcal{M}}^{(0)}|\mathcal{M}^{(0)}\rangle \\ &\qquad\times\frac{e^{\epsilon\gamma}}{2\epsilon\Gamma(1-\epsilon)}H^{(2)}\left[\left(-\frac{\mu^2}{s}\right)^{2\epsilon}+\left(-\frac{\mu^2}{t}\right)^{2\epsilon}-\left(-\frac{\mu^2}{u}\right)^{2\epsilon}\right],\end{aligned} \tag{3.8}$$

where the constant $H^{(2)}$ is

$$H^{(2)} = \left[\frac{1}{4}\gamma_{(1)} + 3C_F K + \frac{5}{2}\zeta_2\beta_0 C_F - \frac{28}{9}\beta_0 C_F - \left(\frac{16}{9} - 7\zeta_3\right) C_F C_A\right]. \tag{3.9}$$

Here ζ_n is the Riemann Zeta function, $\zeta_2 = \pi^2/6$, $\zeta_3 = 1.202056\ldots$ and

$$\gamma_{(1)} = (-3 + 24\zeta_2 - 48\zeta_3)\, C_F^2 + \left(-\frac{17}{3} - \frac{88}{3}\zeta_2 + 24\zeta_3\right) C_F C_A + \left(\frac{4}{3} + \frac{32}{3}\zeta_2\right) C_F T_R N_F. \tag{3.10}$$

The square bracket in Eq. (3.8) is a guess simply motivated by summing over the antennae present in the quark-quark scattering process and on dimensional grounds. Different choices affect only the finite remainder.

The bracket of $\boldsymbol{I}^{(1)}$ between the t-channel tree graph and the finite part of the s-channel one-loop graphs is not symmetric under the exchange of s and t and is given by

$$\begin{aligned}
\langle \overline{\mathcal{M}}^{(0)} | \boldsymbol{I}^{(1)}(\epsilon) | \mathcal{M}^{(1)\mathrm{fin}} \rangle &= \frac{e^{\epsilon\gamma}}{\Gamma(1-\epsilon)} \left(\frac{1}{\epsilon^2} + \frac{3}{2\epsilon}\right) \\
&\times \left\{ \left[\frac{1}{N}\left(-\frac{\mu^2}{s}\right)^{\epsilon} + \frac{1}{N}\left(-\frac{\mu^2}{t}\right)^{\epsilon} - \frac{N^2+1}{N}\left(-\frac{\mu^2}{u}\right)^{\epsilon}\right] \mathcal{F}_1(s,t,u) \right. \\
&\left. + \left[\frac{N^2-1}{N}\left(-\frac{\mu^2}{s}\right)^{\epsilon} - \frac{1}{N}\left(-\frac{\mu^2}{t}\right)^{\epsilon} + \frac{1}{N}\left(-\frac{\mu^2}{u}\right)^{\epsilon}\right] (N^2-1)\, \mathcal{F}_2(s,t,u) \right\}.
\end{aligned} \tag{3.11}$$

The functions $\mathcal{F}_1$ and $\mathcal{F}_2$ appearing in Eq. (3.11) are finite and are given by

$$\begin{aligned}
\mathcal{F}_1(s,t,u) &= \frac{N^2-1}{2N^2}\left[\left(N^2-2\right) f_1(s,t,u) + 2 f_2(s,t,u)\right] \\
&- \frac{1}{2\epsilon\,(3-2\epsilon)}\left[\frac{N^2-1}{N}\left(6 - 7\epsilon - 2\epsilon^2\right) - \frac{1}{N}\left(10\epsilon^2 - 4\epsilon^3\right)\right] \mathrm{Bub}(s) \langle \overline{\mathcal{M}}^{(0)} | \mathcal{M}^{(0)} \rangle \\
&- \frac{e^{\epsilon\gamma}}{\Gamma(1-\epsilon)}\left(\frac{1}{\epsilon^2} + \frac{3}{2\epsilon}\right) \\
&\times \left[\frac{1}{N}\left(-\frac{\mu^2}{s}\right)^{\epsilon} - \frac{2}{N}\left(-\frac{\mu^2}{u}\right)^{\epsilon} - \frac{N^2-2}{N}\left(-\frac{\mu^2}{t}\right)^{\epsilon}\right] \langle \overline{\mathcal{M}}^{(0)} | \mathcal{M}^{(0)} \rangle \\
&- \beta_0 \left[\frac{1}{\epsilon} - \frac{3(1-\epsilon)}{3-2\epsilon}\mathrm{Bub}(s)\right] \langle \overline{\mathcal{M}}^{(0)} | \mathcal{M}^{(0)} \rangle
\end{aligned} \tag{3.12}$$

and

$$\begin{aligned}
\mathcal{F}_2(s,t,u) &= \frac{N^2-1}{2N^2}\Big[f_1(s,t,u) - f_2(s,t,u)\Big] \\
&- \frac{e^{\epsilon\gamma}}{\Gamma(1-\epsilon)}\left(\frac{1}{\epsilon^2} + \frac{3}{2\epsilon}\right)\left[\frac{1}{N}\left(-\frac{\mu^2}{u}\right)^{\epsilon} - \frac{1}{N}\left(-\frac{\mu^2}{t}\right)^{\epsilon}\right] \langle \overline{\mathcal{M}}^{(0)} | \mathcal{M}^{(0)} \rangle
\end{aligned} \tag{3.13}$$

with

$$
\begin{aligned}
f_1(s,t,u) = & \frac{2u}{st}(1-2\epsilon)\left[u^2+t^2-2\epsilon\left(t^2+s^2\right)+\epsilon^2 s^2\right]\mathrm{Box}^6(s,t) \\
& +\frac{2}{st}\left[2u^2-\epsilon\left(5s^2+6t^2+9st\right)+\left(2s^2+4t^2+st\right)\epsilon^2\right. \\
& \qquad \left.+\left(s^2+3st\right)\epsilon^3-st\epsilon^4\right]\left[\frac{\mathrm{Bub}(s)-\mathrm{Bub}(t)}{\epsilon}\right], \qquad (3.14)\\
f_2(s,t,u) = & \frac{2}{s}(1-2\epsilon)\left[2u^2-\epsilon\left(t^2+s^2+u^2\right)+3\epsilon^2 s^2+s^2\epsilon^3\right]\mathrm{Box}^6(s,u) \\
& +\frac{2}{st}\left[2u^2-\epsilon\left(6s^2+6t^2+10st\right)+\left(3s^2+4t^2+3st\right)\epsilon^2\right. \\
& \qquad \left.+\left(s^2+2st\right)\epsilon^3-st\epsilon^4\right]\left[\frac{\mathrm{Bub}(s)-\mathrm{Bub}(u)}{\epsilon}\right]. \qquad (3.15)
\end{aligned}
$$

These expressions are valid in all kinematic regions. However, to evaluate the pole structure in a particular region, they must be expanded as a series in ϵ. We note that in Eq. (3.3) these functions are multiplied by poles in ϵ and must therefore be expanded through to $\mathcal{O}(\epsilon^2)$. In the physical region $u<0$, $t<0$, $\mathrm{Box}^6(u,t)$ has no imaginary part and is given by [23]

$$
\begin{aligned}
\mathrm{Box}^6(u,t) = & \frac{e^{\epsilon\gamma}\Gamma(1+\epsilon)\Gamma(1-\epsilon)^2}{2s\Gamma(1-2\epsilon)(1-2\epsilon)}\left(\frac{\mu^2}{s}\right)^{\epsilon}\left[\frac{1}{2}\left((L_x-L_y)^2+\pi^2\right)\right. \\
& +2\epsilon\left(\mathrm{Li}_3(x)-L_x\mathrm{Li}_2(x)-\frac{1}{3}L_x^3-\frac{\pi^2}{2}L_x\right) \\
& -2\epsilon^2\left(\mathrm{Li}_4(x)+L_y\mathrm{Li}_3(x)-\frac{1}{2}L_x^2\mathrm{Li}_2(x)-\frac{1}{8}L_x^4-\frac{1}{6}L_x^3L_y+\frac{1}{4}L_x^2L_y^2\right. \\
& \left.\left.-\frac{\pi^2}{4}L_x^2-\frac{\pi^2}{3}L_xL_y-\frac{\pi^4}{45}\right)+(u\leftrightarrow t)\right]+\mathcal{O}\left(\epsilon^3\right), \qquad (3.16)
\end{aligned}
$$

where $x=-t/s$, $L_x=\log(x)$ and $L_y=\log(1-x)$ and the polylogarithms $\mathrm{Li}_n(z)$ are defined by

$$
\mathrm{Li}_n(z) = \int_0^z \frac{dt}{t}\mathrm{Li}_{n-1}(t) \qquad \text{for } n=2,3,4 \qquad (3.17)
$$

$$
\mathrm{Li}_2(z) = -\int_0^z \frac{dt}{t}\log(1-t). \qquad (3.18)
$$

Analytic continuation to other kinematic regions is obtained using the inversion formulae for the arguments of the polylogarithms (see for example [29]) when $x>1$

$$
\begin{aligned}
\mathrm{Li}_2(x+i0) &= -\mathrm{Li}_2\left(\frac{1}{x}\right)-\frac{1}{2}\log^2(x)+\frac{\pi^2}{3}+i\pi\log(x) \\
\mathrm{Li}_3(x+i0) &= \mathrm{Li}_3\left(\frac{1}{x}\right)-\frac{1}{6}\log^3(x)+\frac{\pi^2}{3}\log(x)+\frac{i\pi}{2}\log^2(x) \\
\mathrm{Li}_4(x+i0) &= -\mathrm{Li}_4\left(\frac{1}{x}\right)-\frac{1}{24}\log^4(x)+\frac{\pi^2}{6}\log^2(x)+\frac{\pi^4}{45}+\frac{i\pi}{6}\log^3(x). \qquad (3.19)
\end{aligned}
$$

Finally, the one-loop bubble integral in $D = 4 - 2\epsilon$ dimensions is given by

$$\mathrm{Bub}(s) = \frac{e^{\epsilon\gamma}\Gamma\left(1+\epsilon\right)\Gamma\left(1-\epsilon\right)^2}{\Gamma\left(2-2\epsilon\right)\epsilon}\left(-\frac{\mu^2}{s}\right)^{\epsilon}. \tag{3.20}$$

The leading infrared singularity is $\mathcal{O}\left(1/\epsilon^4\right)$ and it is a very stringent check on the reliability of our calculation that the pole structure obtained by computing the Feynman diagrams agrees with that anticipated by Catani through to $\mathcal{O}\left(1/\epsilon\right)$. We therefore construct the finite remainder by subtracting Eq. (3.3) from the full result.

3.2 Finite contributions

In this subsection, we give explicit expressions for the finite two-loop contribution to $\mathcal{B}^8$, $\mathcal{F}inite$, which is given by

$$\mathcal{F}inite = -2\,\mathrm{Re}\left(\langle\mathcal{M}^{(0)}|\overline{\mathcal{M}}^{(2)\,\mathrm{fin}}\rangle + \langle\overline{\mathcal{M}}^{(0)}|\mathcal{M}^{(2)\,\mathrm{fin}}\rangle\right). \tag{3.21}$$

The identical-quark processes probed in high-energy hadron-hadron collisions are the mixed s- and t-channel process

$$q + \bar{q} \to \bar{q} + q,$$

controlled by $\mathcal{B}(s,t,u)$ (as well as the distinct quark matrix elements $\mathcal{A}(s,t,u)$ and $\mathcal{A}(t,s,u)$ as indicated in Eq. (2.10)), and the mixed t- and u-channel processes

$$q + q \to q + q,$$
$$\bar{q} + \bar{q} \to \bar{q} + \bar{q},$$

which are determined by the $\mathcal{B}(t,s,u)$. We need to be able to evaluate the finite parts for each of these processes. Of course, the analytic expressions for different channels are related by crossing symmetry. However, the master crossed boxes have cuts in all three channels yielding complex parts in all physical regions. The analytic continuation is therefore rather involved and prone to error. We therefore choose to give expressions describing $\mathcal{B}^8(s,t,u)$ and $\mathcal{B}^8(t,s,u)$ which are directly valid in the physical region $s > 0$ and $u, t < 0$, and are given in terms of logarithms and polylogarithms that have no imaginary parts.

Using the standard polylogarithm identities [36] we retain the polylogarithms with arguments x, $1-x$ and $(x-1)/x$, where

$$x = -\frac{t}{s}, \qquad y = -\frac{u}{s} = 1 - x, \qquad \frac{x-1}{x} = -\frac{u}{t}. \tag{3.22}$$

For convenience, we also introduce the following logarithms

$$L_x = \log\left(\frac{-t}{s}\right), \qquad L_y = \log\left(\frac{-u}{s}\right), \qquad L_s = \log\left(\frac{s}{\mu^2}\right), \tag{3.23}$$

where μ is the renormalisation scale. The common choice $\mu^2 = s$ corresponds to setting $L_s = 0$.

For each channel, we choose to present our results by grouping terms according to the power of the number of colours N and the number of light quarks N_F, so that in channel c

$$\mathcal{F}inite_c = 2\left(\frac{N^2-1}{N}\right)\left(N^2 A_c + B_c + \frac{1}{N^2}C_c + N N_F D_c + \frac{N_F}{N}E_c + N_F^2 F_c\right). \quad (3.24)$$

Here $c = st$ (ut) to denote the mixed s- and t-channel (u- and t-channel) processes respectively.

3.2.1 The process $q\bar{q} \to \bar{q}q$

We first give expressions for the mixed s-channel and t-channel annihilation process, $q\bar{q} \to \bar{q}q$. We find that

$$\begin{aligned}
A_{st} = \Bigg[& 2\,\mathrm{Li}_4(y) - 2\,\mathrm{Li}_4(x) + 2\,\mathrm{Li}_4\left(\frac{x-1}{x}\right) + \left(-2\,L_x + 12\right)\mathrm{Li}_3(y) + 4\,L_y\,L_x\,\mathrm{Li}_2(y) \\
& + \left(-\frac{23}{3} - 2\,L_x + 4\,L_y\right)\mathrm{Li}_3(x) + \left(\frac{23}{3}\,L_x + 12\,L_y + 2\,L_x^2 + \frac{5}{3}\,\pi^2\right)\mathrm{Li}_2(x) \\
& - \frac{121}{9}\,L_s^2 + \left(\frac{11}{3}\,L_x^2 + \left(-\frac{22}{9} - \frac{22}{3}\,L_y\right)L_x + \frac{11}{3}\,\pi^2 + \frac{22}{3}\,L_y^2 - 22\,L_y + \frac{592}{27}\right)L_s \\
& - \frac{1}{6}\,L_x^4 + \left(\frac{14}{9} + \frac{5}{3}\,L_y\right)L_x^3 + \left(-\frac{11}{12}\,\pi^2 + L_y^2 - \frac{31}{6} + \frac{13}{12}\,L_y\right)L_x^2 \\
& + \left(\frac{1}{3}\,L_y^3 + 6\,L_y^2 + \left(\frac{8}{3}\,\pi^2 + \frac{8}{9}\right)L_y + \frac{89}{36}\,\pi^2 - 6\,\zeta_3 + \frac{695}{216}\right)L_x \\
& - \frac{1}{6}\,L_y^4 + \frac{22}{9}\,L_y^3 + \left(-\frac{169}{18} + \frac{1}{6}\,\pi^2\right)L_y^2 + \left(\frac{61}{18}\,\pi^2 + 12\,\zeta_3 + \frac{1673}{108}\right)L_y \\
& - \frac{347}{18}\,\zeta_3 - \frac{121}{360}\,\pi^4 - \frac{23213}{1296} - \frac{8}{3}\,\pi^2\Bigg]\frac{u^2}{st} \\
& + \Bigg[-4\,\mathrm{Li}_4(x) + 24\,\mathrm{Li}_3(y) + \left(2\,L_x + 12\right)\mathrm{Li}_3(x) + \left(-\frac{2}{3}\,\pi^2 + 24\,L_y - 12\,L_x\right)\mathrm{Li}_2(x) \\
& + \frac{1}{12}\,L_x^4 - \frac{19}{12}\,L_x^3 + \left(-\frac{5}{2} + \frac{1}{3}\,\pi^2\right)L_x^2 + \left(-2\,\zeta_3 - \frac{29}{6}\,\pi^2 + 12\,L_y^2 + 5\,L_y\right)L_x \\
& + \frac{7}{45}\,\pi^4 - \frac{5}{2}\,\pi^2 - 12\,\zeta_3 - 4\,L_y\,\pi^2\Bigg]\frac{u}{s} + \Bigg[3\,L_x^2 + 3\,\pi^2 + 3\,L_y^2 - 6\,L_x\,L_y\Bigg]\frac{t^2}{s^2} + \Bigg[3\,L_y^2\Bigg]\frac{s^2}{t^2} \\
& - 32\,\mathrm{Li}_4(y) - 32\,\mathrm{Li}_4\left(\frac{x-1}{x}\right) + 8\,L_x\,\mathrm{Li}_3(y) + \left(2 - 28\,L_y + 18\,L_x\right)\mathrm{Li}_3(x) \\
& + \left(-2\,L_x^2 + \left(-2 - 24\,L_y\right)L_x - 2\,\pi^2\right)\mathrm{Li}_2(x) - 28\,L_y\,L_x\,\mathrm{Li}_2(y) - \frac{11}{12}\,L_x^4
\end{aligned}$$

$$
\begin{aligned}
&+\left(-\frac{7}{12}+\frac{14}{3}\,L_y\right)L_x^3+\left(-32\,L_y^2+\frac{1}{2}\,L_y+2+\frac{1}{2}\,\pi^2\right)L_x^2\\
&+\left(\left(6+\frac{20}{3}\,\pi^2\right)L_y-\frac{3}{2}\,\pi^2-18\,\zeta_3\right)L_x-2\,\zeta_3-3\,\pi^2-6\,L_y^2+28\,L_y\,\zeta_3+\frac{1}{3}\,\pi^4, \quad (3.25)
\end{aligned}
$$

$$
\begin{aligned}
B_{st}=&\Bigg[-8\,\mathrm{Li}_4(y)-3\,\mathrm{Li}_4(x)-8\,\mathrm{Li}_4\left(\frac{x-1}{x}\right)+8\,L_x\,\mathrm{Li}_3(y)+\left(-6-12\,L_y+12\,L_x\right)\mathrm{Li}_3(x)\\
&+\left(-6\,\pi^2+6\,L_x-\frac{13}{2}\,L_x^2\right)\mathrm{Li}_2(x)-12\,L_y\,L_x\,\mathrm{Li}_2(y)\\
&+\left(-\frac{11}{6}\,L_x^2+\left(-\frac{22}{3}\,L_y+\frac{22}{3}\right)L_x-22\,L_y+\frac{11}{3}\,\pi^2+\frac{22}{3}\,L_y^2+\frac{176}{3}\right)L_s\\
&-\frac{7}{24}\,L_x^4-\frac{7}{9}\,L_x^3+\left(-\frac{17}{2}\,L_y^2+\frac{7}{2}\,L_y-\frac{19}{36}-\frac{1}{6}\,\pi^2\right)L_x^2\\
&+\left(L_y^3-\frac{27}{2}\,L_y^2+\left(-3\,\pi^2+\frac{251}{9}\right)L_y+\frac{181}{9}-\frac{5}{6}\,\pi^2-12\,\zeta_3\right)L_x\\
&-\frac{1}{2}\,L_y^4+\frac{103}{9}\,L_y^3+\left(-\frac{242}{9}+\frac{5}{2}\,\pi^2\right)L_y^2+\left(12\,\zeta_3+\frac{98}{3}+\frac{127}{18}\,\pi^2\right)L_y\\
&+\frac{581}{18}\,\zeta_3-\frac{31}{360}\,\pi^4-\frac{124}{9}\,\pi^2-\frac{30659}{324}\Bigg]\frac{u^2}{st}\\
&+\Bigg[-6\,\mathrm{Li}_4(x)+4\,L_x\,\mathrm{Li}_3(x)-L_x^2\,\mathrm{Li}_2(x)-\frac{22}{3}\,L_x\,L_s-\frac{1}{24}\,L_x^4-\frac{5}{18}\,L_x^3-\frac{47}{3}\,L_x^2\\
&+\left(24\,L_y+\frac{2}{9}\,\pi^2+\frac{128}{9}-4\,\zeta_3\right)L_x+\frac{1}{15}\,\pi^4-\frac{47}{3}\,\pi^2\Bigg]\frac{u}{s}\\
&+\left[-8\,L_x\,L_y+4\,L_x^2+4\,\pi^2+4\,L_y^2\right]\frac{t^2}{s^2}+\left[4\,L_y^2\right]\frac{s^2}{t^2}\\
&+16\,\mathrm{Li}_4(y)+16\,\mathrm{Li}_4\left(\frac{x-1}{x}\right)-16\,L_x\,\mathrm{Li}_3(y)+\left(-12\,L_x+8\,L_y+2\right)\mathrm{Li}_3(x)\\
&+\left(4\,L_x^2+4\,\pi^2-2\,L_x\right)\mathrm{Li}_2(x)+8\,L_y\,L_x\,\mathrm{Li}_2(y)+\frac{11}{3}\,L_x^2\,L_s+\frac{5}{8}\,L_x^4+\left(2-\frac{4}{3}\,L_y\right)L_x^3\\
&+\left(-L_y+4\,L_y^2-\frac{163}{9}\right)L_x^2+\left(\left(\frac{8}{3}\,\pi^2+8\right)L_y+\frac{11}{3}\,\pi^2+12\,\zeta_3\right)L_x\\
&-2\,\zeta_3-\frac{2}{3}\,\pi^4-4\,\pi^2-8\,L_y\,\zeta_3-8\,L_y^2, \qquad (3.26)
\end{aligned}
$$

$$
\begin{aligned}
C_{st}=&\Bigg[-2\,\mathrm{Li}_4(y)-5\,\mathrm{Li}_4(x)-2\,\mathrm{Li}_4\left(\frac{x-1}{x}\right)+2\,L_x\,\mathrm{Li}_3(y)+\left(1+6\,L_x-4\,L_y\right)\mathrm{Li}_3(x)\\
&+\left(-\frac{7}{3}\,\pi^2-\frac{5}{2}\,L_x^2-L_x\right)\mathrm{Li}_2(x)-4\,L_y\,L_x\,\mathrm{Li}_2(y)-\frac{1}{8}\,L_x^4+\left(\frac{5}{12}-\frac{1}{3}\,L_y\right)L_x^3+3\,L_y^3
\end{aligned}
$$

$$
\begin{aligned}
&+\left(\frac{17}{12}\,\pi^2+\frac{5}{4}-\frac{3}{4}\,L_y-\frac{5}{2}\,L_y^2\right)L_x^2+\left(-\frac{9}{2}\,L_y^2+\left(-\frac{5}{3}\,\pi^2+13\right)L_y+\frac{8}{3}\,\pi^2-\frac{45}{8}\right)L_x\\
&+\left(-\frac{21}{2}+\frac{4}{3}\,\pi^2\right)L_y^2+\left(\frac{93}{4}+\frac{13}{6}\,\pi^2-8\,\zeta_3\right)L_y+19\,\zeta_3-\frac{31}{6}\,\pi^2-\frac{511}{16}-\frac{1}{90}\,\pi^4\Bigg]\,\frac{u^2}{st}\\
&+\Bigg[-10\,\mathrm{Li}_4(x)+6\,L_x\,\mathrm{Li}_3(x)+\left(-L_x^2-\frac{2}{3}\,\pi^2\right)\mathrm{Li}_2(x)+\frac{1}{24}\,L_x^4-\frac{13}{12}\,L_x^3\\
&+\left(-\frac{5}{2}+\frac{1}{3}\,\pi^2\right)L_x^2+\left(5\,L_y+\frac{5}{2}\,\pi^2-6\,\zeta_3+12\right)L_x+\frac{2}{9}\,\pi^4-\frac{5}{2}\,\pi^2\Bigg]\,\frac{u}{s}\\
&+\left[L_x^2-2\,L_x\,L_y+\pi^2+L_y^2\right]\frac{t^2}{s^2}+\left[L_y^2\right]\frac{s^2}{t^2}\\
&+8\,\mathrm{Li}_4(y)+8\,\mathrm{Li}_4\left(\frac{x-1}{x}\right)-8\,L_x\,\mathrm{Li}_3(y)+\left(-6\,L_x+4\,L_y+4\right)\mathrm{Li}_3(x)\\
&+\left(-4\,L_x+2\,L_x^2+2\,\pi^2\right)\mathrm{Li}_2(x)+4\,L_y\,L_x\,\mathrm{Li}_2(y)+\frac{13}{24}\,L_x^4+\left(-\frac{5}{12}-\frac{2}{3}\,L_y\right)L_x^3\\
&+\left(-9+2\,L_y^2-\frac{7}{6}\,\pi^2-\frac{1}{2}\,L_y\right)L_x^2+\left(\left(2+\frac{4}{3}\,\pi^2\right)L_y-\frac{3}{2}\,\pi^2+6\,\zeta_3\right)L_x\\
&-4\,\zeta_3-\frac{1}{3}\,\pi^4-2\,L_y^2-4\,L_y\,\zeta_3-\pi^2,
\end{aligned}
\tag{3.27}
$$

$$
\begin{aligned}
D_{st}=&\left[\frac{2}{3}\,\mathrm{Li}_3(x)-\frac{2}{3}\,L_x\,\mathrm{Li}_2(x)+\frac{44}{9}\,L_s^2\right.\\
&+\left(-\frac{2}{3}\,L_x^2+\left(\frac{4}{3}\,L_y+\frac{26}{9}\right)L_x+4\,L_y-\frac{4}{3}\,L_y^2-\frac{389}{27}-\frac{2}{3}\,\pi^2\right)L_s\\
&-\frac{5}{9}\,L_x^3+\left(\frac{2}{3}\,L_y+\frac{37}{18}\right)L_x^2+\left(-\frac{13}{18}\,\pi^2-\frac{11}{9}\,L_y-\frac{40}{9}\right)L_x-\frac{4}{9}\,L_y^3+\frac{29}{9}\,L_y^2\\
&\left.+\left(-\frac{11}{9}\,\pi^2-\frac{149}{27}\right)L_y-\frac{2}{9}\,\pi^2+\frac{43}{9}\,\zeta_3+\frac{455}{27}\right]\frac{u^2}{st},
\end{aligned}
\tag{3.28}
$$

$$
\begin{aligned}
E_{st}=&\left[2\,\mathrm{Li}_3(x)-2\,L_x\,\mathrm{Li}_2(x)+\left(\frac{1}{3}\,L_x^2+\left(\frac{4}{3}\,L_y-\frac{4}{3}\right)L_x-\frac{2}{3}\,\pi^2-\frac{4}{3}\,L_y^2+4\,L_y-\frac{29}{3}\right)L_s\right.\\
&+\frac{1}{9}\,L_x^3-\frac{19}{18}\,L_x^2+\left(-\frac{11}{9}\,L_y+\frac{1}{3}\,\pi^2-\frac{43}{9}\right)L_x-\frac{4}{9}\,L_y^3+\frac{29}{9}\,L_y^2+\left(-\frac{14}{9}\,\pi^2-\frac{11}{3}\right)L_y\\
&\left.+\frac{29}{9}\,\zeta_3+\frac{1370}{81}+\frac{22}{9}\,\pi^2\right]\frac{u^2}{st}\\
&+\left[\frac{4}{3}\,L_x\,L_s+\frac{1}{9}\,L_x^3+\frac{2}{3}\,L_x^2+\left(-\frac{2}{9}\,\pi^2-\frac{32}{9}\right)L_x+\frac{2}{3}\,\pi^2\right]\frac{u}{s}\\
&-\frac{1}{3}\,L_x^3+\frac{16}{9}\,L_x^2-\frac{2}{3}\,L_x\,\pi^2-\frac{2}{3}\,L_x^2\,L_s,
\end{aligned}
\tag{3.29}
$$

$$
F_{st}=\left[-\frac{4}{9}\,L_s^2+\left(\frac{40}{27}-\frac{4}{9}\,L_x\right)L_s+\frac{2}{9}\,\pi^2-\frac{100}{81}+\frac{20}{27}\,L_x-\frac{2}{9}\,L_x^2\right]\frac{u^2}{st}. \tag{3.30}
$$

Some of these results overlap with the analytic expressions presented in Ref. [23] for the QED process $e^+e^- \to e^+e^-$. To obtain the QED limit from a QCD calculation corresponds to setting $C_A = 0$, $C_F = 1$, $T_R = 1$ as well as setting the cubic Casimir $C_3 = (N^2-1)(N^2-2)/N^2$ to 0. This means that we can directly compare $E_{st}(\propto C_F T_R N_F)$ and $F_{st}(\propto T_R^2 N_F^2)$ but *not* C_{st} which receives contributions from both C_3 and C_F^2. We see that (3.29) and (3.30) agree with Eqs. (2.50) and (2.51) of [23] respectively.

The other coefficients, A_{st}, B_{st}, C_{st} and D_{st} are new results.

3.2.2 The process $q+q \to q+q$

The mixed t- and u-channel process, $q+q \to q+q$ is fixed by $\mathcal{B}^8(t,s,u)$. We find that the finite two-loop contribution is given by Eq. (3.24) with

$$
\begin{aligned}
A_{ut} = {}& \Bigg[2\,\mathrm{Li}_4\left(\frac{x-1}{x}\right) - 2\,\mathrm{Li}_4(x) - 2\,\mathrm{Li}_4(y) + \left(2\,L_x + 2\,L_y + \frac{23}{3}\right)\mathrm{Li}_3(x) + \left(4\,L_y + \frac{59}{3}\right)\mathrm{Li}_3(y) \\
&+\left(-2\,L_x^2 + \left(-\frac{23}{3} + 2\,L_y\right)L_x + \frac{1}{3}\pi^2 + \frac{59}{3}\,L_y\right)\mathrm{Li}_2(x) + \left(2\,L_x\,L_y - 2\,L_y^2\right)\mathrm{Li}_2(y) \\
&-\frac{121}{9}\,L_s^2 + \left(\frac{11}{3}\,L_x^2 + \frac{592}{27} - \frac{22}{9}\,L_y - \frac{22}{9}\,L_x + \frac{11}{3}\,L_y^2\right)L_s - \frac{1}{6}\,L_x^4 + \left(-\frac{4}{3}\,L_y + \frac{14}{9}\right)L_x^3 \\
&+\left(-\frac{25}{12}\,L_y - \frac{31}{6} + \frac{7}{12}\pi^2 + \frac{7}{2}\,L_y^2\right)L_x^2 - \frac{1}{3}\,L_y^4 + \frac{113}{36}\,L_y^3 + \left(-\frac{8}{3} + \frac{7}{12}\pi^2\right)L_y^2 \\
&+\left(-\frac{2}{3}\,L_y^3 + \frac{77}{6}\,L_y^2 + \left(7 - \frac{17}{6}\pi^2\right)L_y + \frac{695}{216} + \frac{59}{36}\pi^2 - 8\,\zeta_3\right)L_x \\
&+\left(\frac{695}{216} - 8\,\zeta_3 - \frac{73}{18}\pi^2\right)L_y - \frac{23213}{1296} + \frac{17}{24}\pi^4 - \frac{485}{18}\,\zeta_3 + \frac{73}{18}\pi^2\Bigg]\frac{s^2}{ut} \\
&+\Bigg[4\,\mathrm{Li}_4\left(\frac{x-1}{x}\right) + \left(-2\,L_x + 2\,L_y - 12\right)\mathrm{Li}_3(x) + \left(2\,L_y + 12 - 2\,L_x\right)\mathrm{Li}_3(y) \\
&+\left(\left(2\,L_y + 12\right)L_x + \frac{2}{3}\pi^2 + 12\,L_y\right)\mathrm{Li}_2(x) + 2\,L_y\,L_x\,\mathrm{Li}_2(y) + \frac{1}{4}\,L_x^4 + \left(-L_y - \frac{19}{12}\right)L_x^3 \\
&+\left(-\frac{5}{2} + \frac{1}{6}\pi^2 + \frac{5}{2}\,L_y^2 + \frac{19}{4}\,L_y\right)L_x^2 + \left(\frac{29}{4}\,L_y^2 - \frac{1}{3}\,L_y\,\pi^2 + \frac{29}{12}\pi^2 + \frac{1}{3}\,L_y^3\right)L_x \\
&-\frac{1}{12}\,L_y^4 + \frac{19}{12}\,L_y^3 + \left(\frac{1}{6}\pi^2 + \frac{5}{2}\right)L_y^2 - \frac{53}{12}\,L_y\,\pi^2 - \frac{1}{60}\pi^4\Bigg]\frac{s}{u} + \Big[3\,L_x^2\Big]\frac{t^2}{u^2} + \Big[3\,L_y^2\Big]\frac{u^2}{t^2} \\
&+32\,\mathrm{Li}_4(x) + 32\,\mathrm{Li}_4(y) + \left(-18\,L_x - 10\,L_y - 2\right)\mathrm{Li}_3(x) + \left(-2 - 10\,L_x - 18\,L_y\right)\mathrm{Li}_3(y) \\
&+\left(2\,L_x^2 + \left(2 - 10\,L_y\right)L_x - 2\,L_y\right)\mathrm{Li}_2(x) + \left(-10\,L_x\,L_y + 2\,L_y^2\right)\mathrm{Li}_2(y) \\
&+\frac{5}{12}\,L_x^4 + \left(-L_y - \frac{7}{12}\right)L_x^3 + \left(2 - \frac{27}{2}\,L_y^2 + \frac{5}{4}\,L_y - \frac{4}{3}\pi^2\right)L_x^2
\end{aligned}
$$

$$
+\Big(- L_y^3 - \frac{3}{4}\, L_y^2 + \Big(- 10 + 6\,\pi^2\Big)\, L_y - \frac{1}{4}\,\pi^2\Big)\, L_x + \frac{5}{12}\, L_y^4 - \frac{7}{12}\, L_y^3 + \Big(2 - \frac{4}{3}\,\pi^2\Big)\, L_y^2
$$

$$
+\frac{1}{12}\, L_y\,\pi^2 - \frac{391}{180}\,\pi^4 + 5\,\pi^2, \tag{3.31}
$$

$$
\begin{aligned}
B_{ut} = & \Big[3\,\mathrm{Li}_4\Big(\frac{x-1}{x}\Big) + 8\,\mathrm{Li}_4(x) + 8\,\mathrm{Li}_4(y) + \Big(- 12\, L_x + 6\Big)\,\mathrm{Li}_3(x) + \Big(6 - 8\, L_y - 4\, L_x\Big)\,\mathrm{Li}_3(y) \\
& + \Big(\frac{13}{2}\, L_x^2 + \Big(- 6 - L_y\Big)\, L_x + 6\, L_y + \frac{1}{2}\,\pi^2\Big)\,\mathrm{Li}_2(x) + \frac{11}{2}\, L_y^2\,\mathrm{Li}_2(y) \\
& + \Big(- \frac{11}{6}\, L_x^2 + \Big(11\, L_y + \frac{22}{3}\Big)\, L_x - \frac{11}{6}\, L_y^2 + \frac{176}{3} + \frac{44}{3}\, L_y - \frac{11}{2}\,\pi^2\Big)\, L_s + \frac{1}{6}\, L_x^4 \\
& + \Big(- \frac{7}{9} + \frac{2}{3}\, L_y\Big)\, L_x^3 + \Big(- 3\, L_y + 4\,\pi^2 - \frac{19}{36} - \frac{1}{4}\, L_y^2\Big)\, L_x^2 + \frac{1}{12}\, L_y^4 \\
& + \Big(L_y^3 + \frac{13}{6}\, L_y^2 + \Big(- \frac{39}{2} - \frac{1}{3}\,\pi^2\Big)\, L_y + \frac{181}{9} + \frac{53}{6}\,\pi^2\Big)\, L_x - \frac{1}{2}\, L_y^3 \\
& + \Big(\frac{545}{36} + 4\,\pi^2\Big)\, L_y^2 + \Big(\frac{53}{9} + \frac{76}{9}\,\pi^2\Big)\, L_y - \frac{161}{120}\,\pi^4 - \frac{30659}{324} + \frac{473}{18}\,\zeta_3 + \frac{113}{4}\,\pi^2\Big]\,\frac{s^2}{ut} \\
& + \Big[6\,\mathrm{Li}_4\Big(\frac{x-1}{x}\Big) + \Big(4\, L_y - 4\, L_x\Big)\,\mathrm{Li}_3(x) + \Big(4\, L_y - 4\, L_x\Big)\,\mathrm{Li}_3(y) \\
& + \Big(L_x^2 + \pi^2 + 2\, L_x\, L_y\Big)\,\mathrm{Li}_2(x) + \Big(- L_y^2 + 4\, L_x\, L_y\Big)\,\mathrm{Li}_2(y) + \Big(\frac{22}{3}\, L_y - \frac{22}{3}\, L_x\Big)\, L_s \\
& + \frac{5}{24}\, L_x^4 + \Big(- \frac{5}{18} - \frac{5}{6}\, L_y\Big)\, L_x^3 + \Big(- \frac{47}{3} + \frac{5}{6}\, L_y + \frac{1}{4}\,\pi^2 + \frac{15}{4}\, L_y^2\Big)\, L_x^2 \\
& + \Big(\frac{128}{9} - \frac{1}{6}\, L_y^3 - \frac{11}{18}\,\pi^2 - \frac{1}{2}\, L_y\,\pi^2 - \frac{5}{6}\, L_y^2\Big)\, L_x + \frac{1}{24}\, L_y^4 + \frac{5}{18}\, L_y^3 + \Big(\frac{47}{3} + \frac{1}{4}\,\pi^2\Big)\, L_y^2 \\
& + \Big(- \frac{128}{9} + \frac{11}{18}\,\pi^2\Big)\, L_y - \frac{1}{40}\,\pi^4\Big]\,\frac{s}{u} + \Big[4\, L_x^2\Big]\,\frac{t^2}{u^2} + \Big[4\, L_y^2\Big]\,\frac{u^2}{t^2} \\
& - 16\,\mathrm{Li}_4(x) - 16\,\mathrm{Li}_4(y) + \Big(12\, L_x - 4\, L_y - 2\Big)\,\mathrm{Li}_3(x) + \Big(- 4\, L_x - 2 + 12\, L_y\Big)\,\mathrm{Li}_3(y) \\
& + \Big(- 4\, L_x^2 + \Big(2 - 4\, L_y\Big)\, L_x - 2\, L_y\Big)\,\mathrm{Li}_2(x) + \Big(- 4\, L_y^2 - 4\, L_x\, L_y\Big)\,\mathrm{Li}_2(y) \\
& + \Big(\frac{11}{3}\, L_y^2 + \frac{11}{3}\, L_x^2 + \frac{11}{3}\,\pi^2 - \frac{22}{3}\, L_x\, L_y\Big)\, L_s - \frac{1}{24}\, L_x^4 + \Big(- \frac{7}{6}\, L_y + 2\Big)\, L_x^3 \\
& + \Big(\frac{5}{12}\,\pi^2 - \frac{163}{9} - \frac{17}{4}\, L_y^2 - \frac{4}{3}\, L_y\Big)\, L_x^2 + \Big(- \frac{7}{6}\, L_y^3 - \frac{10}{3}\, L_y^2 + \Big(\frac{1}{2}\,\pi^2 + \frac{254}{9}\Big)\, L_y + \frac{7}{3}\,\pi^2\Big)\, L_x \\
& - \frac{1}{24}\, L_y^4 + 2\, L_y^3 + \Big(\frac{5}{12}\,\pi^2 - \frac{163}{9}\Big)\, L_y^2 + \frac{8}{3}\, L_y\,\pi^2 + \frac{421}{360}\,\pi^4 - \frac{127}{9}\,\pi^2,
\end{aligned} \tag{3.32}
$$

$$
C_{ut} = \Big[5\,\mathrm{Li}_4\Big(\frac{x-1}{x}\Big) + 2\,\mathrm{Li}_4(x) + 2\,\mathrm{Li}_4(y) + \Big(2\, L_y - 6\, L_x - 1\Big)\,\mathrm{Li}_3(x) + \Big(- 4\, L_x - 1\Big)\,\mathrm{Li}_3(y)
$$

$$
\begin{aligned}
&+\left(\frac{5}{2}\,L_x^2+\left(1+L_y\right)L_x-L_y+\frac{5}{6}\,\pi^2\right)\mathrm{Li}_2(x)+\left(2\,L_x\,L_y+\frac{3}{2}\,L_y^2\right)\mathrm{Li}_2(y)\\
&+\frac{1}{6}\,L_x^4+\frac{5}{12}\,L_x^3+\left(\frac{7}{4}\,\pi^2-\frac{1}{2}\,L_y+\frac{5}{4}+\frac{5}{4}\,L_y^2\right)L_x^2-\frac{1}{12}\,L_y^4+\frac{3}{2}\,L_y^3\\
&+\left(L_y^3-\frac{19}{4}\,L_y^2+\left(-\frac{5}{6}\,\pi^2-\frac{31}{2}\right)L_y+\frac{41}{12}\,\pi^2+6\,\zeta_3-\frac{45}{8}\right)L_x+\left(\frac{7}{4}\,\pi^2+\frac{15}{4}\right)L_y^2\\
&+\left(-\frac{141}{8}+6\,\zeta_3+\frac{13}{3}\,\pi^2\right)L_y-\frac{511}{16}+20\,\zeta_3+\frac{109}{12}\,\pi^2-\frac{49}{90}\,\pi^4\Bigg]\,\frac{s^2}{ut}\\
&+\Bigg[10\,\mathrm{Li}_4\!\left(\frac{x-1}{x}\right)+\left(-6\,L_x+6\,L_y\right)\mathrm{Li}_3(x)+\left(-6\,L_x+6\,L_y\right)\mathrm{Li}_3(y)\\
&+\left(L_x^2+4\,L_x\,L_y+\frac{5}{3}\,\pi^2\right)\mathrm{Li}_2(x)+\left(6\,L_x\,L_y-L_y^2\right)\mathrm{Li}_2(y)+\frac{11}{24}\,L_x^4+\left(-\frac{11}{6}\,L_y-\frac{13}{12}\right)L_x^3\\
&+\left(\frac{25}{4}\,L_y^2+\frac{13}{4}\,L_y+\frac{5}{12}\,\pi^2-\frac{5}{2}\right)L_x^2+\left(-\frac{3}{4}\,\pi^2+12+\frac{1}{6}\,L_y^3-\frac{13}{4}\,L_y^2-\frac{5}{6}\,L_y\,\pi^2\right)L_x\\
&-\frac{1}{24}\,L_y^4+\frac{13}{12}\,L_y^3+\left(\frac{5}{2}+\frac{5}{12}\,\pi^2\right)L_y^2+\left(-12+\frac{3}{4}\,\pi^2\right)L_y-\frac{1}{24}\,\pi^4\Bigg]\,\frac{s}{u}+\Big[L_x^2\Big]\,\frac{t^2}{u^2}\\
&+\Big[L_y^2\Big]\,\frac{u^2}{t^2}-8\,\mathrm{Li}_4(x)-8\,\mathrm{Li}_4(y)+\left(6\,L_x-2\,L_y-4\right)\mathrm{Li}_3(x)+\left(-4-2\,L_x+6\,L_y\right)\mathrm{Li}_3(y)\\
&+\left(-2\,L_x^2+\left(4-2\,L_y\right)L_x-4\,L_y\right)\mathrm{Li}_2(x)+\left(-2\,L_x\,L_y-2\,L_y^2\right)\mathrm{Li}_2(y)\\
&+\frac{5}{24}\,L_x^4+\left(-\frac{3}{2}\,L_y-\frac{5}{12}\right)L_x^3+\left(-9-\frac{3}{4}\,L_y^2+\frac{7}{4}\,L_y+\frac{5}{12}\,\pi^2\right)L_x^2\\
&+\left(-\frac{3}{2}\,L_y^3-\frac{9}{4}\,L_y^2+\left(16-\frac{1}{6}\,\pi^2\right)L_y+\frac{1}{4}\,\pi^2\right)L_x+\frac{5}{24}\,L_y^4-\frac{5}{12}\,L_y^3+\left(-9+\frac{5}{12}\,\pi^2\right)L_y^2\\
&+\frac{11}{12}\,L_y\,\pi^2+\frac{203}{360}\,\pi^4-8\,\pi^2, \qquad (3.33)
\end{aligned}
$$

$$
\begin{aligned}
D_{ut} =\ &\Bigg[-\frac{2}{3}\,\mathrm{Li}_3(x)-\frac{2}{3}\,\mathrm{Li}_3(y)+\left(-\frac{2}{3}\,L_y+\frac{2}{3}\,L_x\right)\mathrm{Li}_2(x)+\frac{44}{9}\,L_s^2\\
&+\left(\frac{26}{9}\,L_x-\frac{2}{3}\,L_x^2+\frac{26}{9}\,L_y-\frac{389}{27}-\frac{2}{3}\,L_y^2\right)L_s-\frac{5}{9}\,L_x^3+\left(\frac{37}{18}+\frac{1}{3}\,L_y\right)L_x^2\\
&+\left(-\frac{7}{18}\,\pi^2-\frac{1}{3}\,L_y^2-\frac{40}{9}\right)L_x-\frac{5}{9}\,L_y^3+\frac{37}{18}\,L_y^2+\left(-\frac{40}{9}-\frac{5}{18}\,\pi^2\right)L_y\\
&+\frac{49}{9}\,\zeta_3-\frac{25}{18}\,\pi^2+\frac{455}{27}\Bigg]\,\frac{s^2}{ut}, \qquad (3.34)
\end{aligned}
$$

$$
E_{ut} = \Bigg[-2\,\mathrm{Li}_3(x)-2\,\mathrm{Li}_3(y)+\left(-2\,L_y+2\,L_x\right)\mathrm{Li}_2(x)+\frac{1}{9}\,L_x^3-\frac{19}{18}\,L_x^2
$$

$$
\begin{aligned}
&+\left(\frac{1}{3}\,L_x^2+\left(-2\,L_y-\frac{4}{3}\right)L_x-\frac{29}{3}+\frac{1}{3}\,L_y^2+\pi^2-\frac{8}{3}\,L_y\right)L_s\\
&+\left(-\frac{5}{3}\,L_y^2+2\,L_y+\frac{2}{3}\,\pi^2-\frac{43}{9}\right)L_x-\frac{31}{18}\,L_y^2+\left(\frac{8}{9}\,\pi^2-\frac{11}{9}\right)L_y\\
&+\frac{1370}{81}-\frac{5}{2}\,\pi^2+\frac{47}{9}\,\zeta_3\Bigg]\,\frac{s^2}{ut}\\
&+\Bigg[\left(\frac{4}{3}\,L_x-\frac{4}{3}\,L_y\right)L_s+\frac{1}{9}\,L_x^3+\left(-\frac{1}{3}\,L_y+\frac{2}{3}\right)L_x^2+\left(\frac{1}{3}\,L_y^2+\frac{1}{9}\,\pi^2-\frac{32}{9}\right)L_x\\
&-\frac{1}{9}\,L_y^3-\frac{2}{3}\,L_y^2+\left(-\frac{1}{9}\,\pi^2+\frac{32}{9}\right)L_y\Bigg]\,\frac{s}{u}\\
&+\left(-\frac{2}{3}\,L_y^2-\frac{2}{3}\,L_x^2-\frac{2}{3}\,\pi^2+\frac{4}{3}\,L_x\,L_y\right)L_s-\frac{1}{3}\,L_x^3+\left(\frac{1}{3}\,L_y+\frac{16}{9}\right)L_x^2\\
&+\left(-\frac{32}{9}\,L_y+\frac{1}{3}\,L_y^2-\frac{1}{3}\,\pi^2\right)L_x+\frac{16}{9}\,L_y^2-\frac{1}{3}\,L_y^3+\frac{16}{9}\,\pi^2-\frac{1}{3}\,L_y\,\pi^2, \qquad (3.35)
\end{aligned}
$$

$$
F_{ut}=\left[-\frac{4}{9}\,L_s^2+\left(-\frac{4}{9}\,L_y+\frac{40}{27}-\frac{4}{9}\,L_x\right)L_s+\frac{20}{27}\,L_x-\frac{2}{9}\,L_x^2+\frac{20}{27}\,L_y-\frac{2}{9}\,L_y^2-\frac{100}{81}\right]\frac{s^2}{ut}. \qquad (3.36)
$$

As in Section 3.2.1, we can compare some of these results with the analytic expressions presented in Ref. [23] for the QED process $e^+e^- \to e^+e^-$, and we see that (3.35) and (3.36) agree with Eqs. (2.55) and (2.56) of [23] respectively.

The other coefficients, A_{ut}, B_{ut}, C_{ut} and D_{ut} represent new results.

4. Summary

In this paper we discussed the two-loop QCD corrections to the scattering of two identical massless quarks. For the annihilation process, both s-channel and t-channel graphs are present. The interference of s-channel tree and two-loop graphs is determined by $\mathcal{A}^{8(2\times0)}(s,t,u)$ which is the same function that describes distinct quark scattering in the s-channel. Similarly, the interference of the t-channel tree and two-loop graphs is fixed by $\mathcal{A}^{8(2\times0)}(t,s,u)$. Explicit expressions for $\mathcal{A}^{8(2\times0)}$ are given in [24]. The modification to the matrix elements due to the interference of the s-channel tree graph with the t-channel two-loop graphs (and vice versa) is represented by $\mathcal{B}^{8(2\times0)}(s,t,u)$ (see Eq. (2.10)). To obtain $\mathcal{B}^{8(2\times0)}$, we have used conventional dimensional regularisation and the $\overline{\mathrm{MS}}$ renormalisation scheme to compute the interference of the tree and two-loop graphs summed over spins and colours.

The pole structure for $\mathcal{B}^{8(2\times0)}(s,t,u)$ is given in Eq. (3.3) while expressions for the finite parts are given for the mixed s- and t-channels and mixed u- and t-channels in

Secs. 3.2.1 and 3.2.2 respectively. Together with the analogous expressions for unlike-quark scattering given in Ref. [24], they complete the analytic formulae required to describe the two-loop contribution to quark-quark scattering through to $\mathcal{O}(\epsilon^0)$.

These results form an important part of the next-to-next-to-leading order predictions for jet cross sections in hadron-hadron collisions. However, they are only a part of the whole and must be combined with the tree-level $2 \to 4$, the one-loop $2 \to 3$ as well as the square of the one-loop $2 \to 2$ processes to yield physical cross sections. For the most part, the matrix elements themselves are available in the literature. Each of the contributions is divergent in the infrared limit and a systematic procedure for analytically canceling the infrared divergences needs to be established for semi-inclusive jet cross sections. Recent progresses in determining the singular limits of tree-level matrix elements when two particles are unresolved [37, 38] and the soft and collinear limits of one-loop amplitudes [39, 40], together with the analytic cancellation of the infrared singularities in the somewhat simpler case of $e^+e^- \to$ photon+jet at next-to-leading order [41], suggest that the technical problems will soon be solved for generic $2 \to 2$ scattering processes. There are additional problems due to initial state radiation. However, the recent steps taken towards the determination of the three-loop splitting functions [12, 13, 14] are also promising. We therefore expect that the problem of the analytic cancellation of the infrared divergences will soon be addressed thereby enabling the construction of numerical programs to provide next-to-next-to-leading order QCD estimates of jet production in hadron collisions.

Acknowledgements

C.A. acknowledges the financial support of the Greek Government and M.E.T. acknowledges financial support from CONACyT and the CVCP. We gratefully acknowledge the support of the British Council and German Academic Exchange Service under ARC project 1050. This work was supported in part by the EU Fourth Framework Programme 'Training and Mobility of Researchers', Network 'Quantum Chromodynamics and the Deep Structure of Elementary Particles', contract FMRX-CT98-0194 (DG-12-MIHT).

References

[1] S.D. Ellis, Z. Kunzst and D.E. Soper, Phys. Rev. Lett. **69** (1992) 3615 [hep-ph/9208249].

[2] W.T. Giele, E.W.N. Glover and D.A. Kosower, Phys.Rev. **D52** (1995) 1486 [hep-ph/9412338].

[3] F. Abe et al., CDF Collaboration, Phys. Rev. Lett. **77** (1996) 438 [hep-ex/9601008].

[4] B. Abbott et al., D0 Collaboration, Phys. Rev. Lett. **82** (1999) 2451 [hep-ex/9807018].

[5] Z. Bern, L. Dixon, D.A. Kosower, Phys. Rev. Lett **70** (1993) 2677 [hep-ph/9302280].

[6] Z. Bern, L. Dixon and D.A. Kosower, Nucl. Phys. **B437** (1995) 259 [hep-ph/9409393].

[7] Z. Kunszt, A. Signer and Z. Trócsányi, *Phys. Lett* **B336** (1994) 529 [hep-ph/9405386].

[8] J.F. Gunion and J. Kalinowski, Phys. Rev. **D34** (1986) 2119;
S.J. Parke and T.R. Taylor, Nucl. Phys. **B269** (1986) 410;
F.A. Berends and W.T. Giele, Nucl. Phys. **B294** (1987) 700;
M. Mangano, S.J. Parke and Z. Xu, Nucl. Phys. **B298** (1988) 653.

[9] Z. Kunszt, Nucl. Phys. **B271** (1986) 333;
S.J. Parke and T.J. Taylor, Phys. Rev. **D35** (1987) 313.

[10] J.F. Gunion and Z. Kunszt, Phys. Lett. **159B** (1985) 167.

[11] J.F. Gunion and Z. Kunszt, Phys. Lett. **176B** (1986) 163.

[12] S.A. Larin, T. van Ritbergen, and J.A.M. Vermaseren, Nucl. Phys. **B427** (1994) 41;
S.A. Larin, P. Nogueira, T. van Ritbergen, and J.A.M. Vermaseren, Nucl. Phys. **B492** (1997) 338 [hep-ph/9605317].

[13] A. Retey and J.A.M. Vermaseren, `hep-ph/0007294`.

[14] J. A. Gracey, Phys. Lett. **B322** (1994) 141 [hep-ph/9401214].

[15] W.L. van Neerven and A. Vogt, Nucl. Phys. **B568** (2000) 263 [hep-ph/9907472]; `hep-ph/0006154`.

[16] W.L. van Neerven and A. Vogt, Phys. Lett. **B490** (2000) 111 [hep-ph/0007362].

[17] A.D. Martin, R.G. Roberts, W.J. Stirling and R.S. Thorne, hep-ph/0007099.

[18] V.A. Smirnov, Phys. Lett. **B460** (1999) 397 [hep-ph/9905323].

[19] J.B. Tausk, Phys. Lett. **B469** (1999) 225 [hep-ph/9909506].

[20] V.A. Smirnov and O.L. Veretin, Nucl. Phys. **B566** (2000) 469 [hep-ph/9907385].

[21] C. Anastasiou, T. Gehrmann, C. Oleari, E. Remiddi and J.B. Tausk, Nucl. Phys. **B580** (2000) 577 [hep-ph/0003261].

[22] Z. Bern, L. Dixon and D.A. Kosower, JHEP **0001** (2000) 027 [hep-ph/0001001].

[23] Z. Bern, L. Dixon and A. Ghinculov, hep-ph/0010075.

[24] C. Anastasiou, E.W.N. Glover, C. Oleari and M.E. Tejeda-Yeomans, hep-ph/0010212.

[25] S. Catani, Phys. Lett. **B427** (1998) 161 [hep-ph/9802439].

[26] R.K. Ellis and J.C. Sexton, Nucl. Phys. **B269** (1986) 445.

[27] P. Nogueira, J.Comput.Phys. **105** (1993) 279.

[28] C. Anastasiou, E.W.N. Glover and C. Oleari, Nucl. Phys. **B572** (2000) 307 [hep-ph/9907494].

[29] C. Anastasiou, E.W.N. Glover and C. Oleari, Nucl. Phys. **B575** (2000) 416, Erratum-ibid. **B585** (2000) 763 [hep-ph/9912251].

[30] K.G. Chetyrkin, A.L. Kataev and F.V. Tkachov, Nucl. Phys. **B174** (1980) 345 ;
K.G. Chetyrkin and F.V. Tkachov, Nucl. Phys. **B192** (1981) 159.

[31] T. Gehrmann and E. Remiddi, Nucl. Phys. **B580** (2000) 485 [hep-ph/9912329].

[32] E.W.N. Glover and M.E. Tejeda-Yeomans, Nucl. Phys. Proc. Suppl. **89** (2000) 196 [hep-ph/0010031].

[33] R.J. Gonsalves, Phys. Rev. **D28** (1983) 1542;
G. Kramer and B. Lampe, J. Math. Phys. **28** (1987) 945.

[34] T. Gehrmann and E. Remiddi, Nucl. Phys. Proc. Suppl. **89** (2000) 2512 [hep-ph/0005232].

[35] C. Anastasiou, J.B. Tausk and M.E. Tejeda-Yeomans, Nucl. Phys. Proc. Suppl. **89** (2000) 262 [hep-ph/0005328].

[36] K.S. Kölbig, J.A. Mignaco and E. Remiddi, *B.I.T.* **10** (1970) 38.

[37] J.M. Campbell and E.W.N. Glover, Nucl. Phys. **B527** (1998) 264 [hep-ph/9710255];
S. Catani and M. Grazzini, Phys. Lett. **446B** (1999) 143 [hep-ph/9810389], Nucl. Phys. **B570** (2000) 287 [hep-ph/9908523].

[38] F.A. Berends and W.T. Giele, Nucl. Phys. **B313** (1989) 595;
S. Catani, in Proceedings of the workshop on *New Techniques for Calculating Higher Order QCD Corrections*, report ETH-TH/93-01, Zurich (1992).

[39] Z. Bern, V. Del Duca and C.R. Schmidt, Phys. Lett. **445B** (1998) 168 [hep-ph/9810409];
Z. Bern, V. Del Duca, W.B. Kilgore and C.R. Schmidt, Phys. Rev. **D60** (1999) 116001 [hep-ph/9903516];
S. Catani and M. Grazzini, hep-ph/0007142.

[40] Z. Bern, L. Dixon, D.C. Dunbar and D.A. Kosower, Nucl. Phys. **B425** (1994) 217 [hep-ph/9403226];
D.A. Kosower, Nucl. Phys. **B552** (1999) 319;
D.A. Kosower and P. Uwer, Nucl. Phys. **B563** (1999) 477 [hep-ph/9903515].

[41] A. Gehrmann-De Ridder and E.W.N. Glover, Nucl. Phys. **B517** (1998) 269 [hep-ph/9707224].